Phase ordering kinetics in the Swift-Hohenberg equation

Katsuya Ouchi
Kobe Design University, 8-1-1 Gakuennishi-machi, Nishi-ku, Kobe 651-21, Japan

Hirokazu Fujisaka
Department of Physics, Kyushu University 33, Fukuoda 812-81, Japan

(Received 28 December 1995)

It is shown that the Swift-Hohenberg equation $\dot{w}=\epsilon w-(\nabla^2+k_0^2)^2 w-w^3$ for $\epsilon>3/2k_0^4$ exhibits a new phase ordering kinetics from the lamellar phase to the uniform state. A domain wall propagates with the velocity $c(R)=-(2/R)(\epsilon+8k_0^4)/4k_0^2$ and reduces the domain structure which finally shrinks to a spot. Here R^{-1} denotes the curvature of the domain wall. The dynamics of relaxation is investigated by observing how the structure function evolves in time. It is found that the structure function shows the same scaling relationship that is known from the ordering kinetics in the time-dependent Ginzburg-Landau equation. [S1063-651X(96)11509-9]

PACS number(s): 82.20.Wt, 05.70.Ln, 82.40.−g, 82.20.Mj

In recent years, pattern formation in systems far from equilibrium have been extensively studied from the numerical as well as experimental point of view [2], e.g., the Rayleigh-Bénard convection for liquid layers heated from below [1,2], liquid crystals under an electric field [3,4], chemical reaction-diffusion systems [5,6], etc. Especially, stationary inhomogeneous patterns arising through symmetry breaking instability have been observed recently in experiments by using an open, unstirred chemical reactor (gel reactor), which produces spatially inhomogeneous states (Turing patterns). Ouyang and Swinney found bifurcations among several patterns and showed that roll, hexagon, and their mixed states are formed depending on the external control parameters [6].

The dynamics near the onset of the pattern formation is often discussed with the Swift-Hohenberg (SH) equation [7–9],

$$\frac{\partial w(\mathbf{r},t)}{\partial t}=[\epsilon-(\nabla^2+k_0^2)^2]w-w^3=-\frac{\delta H\{w\}}{\delta w(\mathbf{r},t)}, \quad (1)$$

where

$$H\{w\}=\int d\mathbf{r}\left[-\frac{\epsilon}{2}w^2+\frac{1}{4}w^4+\frac{1}{2}\{(\nabla^2+k_0^2)w\}^2\right]. \quad (2)$$

The SH equation has been derived by carrying out the perturbation expansion with respect to the deviation from the heat conduction state in a Rayleigh-Bénard system [10]. The value of H decreases monotonously in time

$$\dot{H}=-\int\left(\frac{\delta H}{\delta w}\right)^2 d\mathbf{r}\leqslant 0. \quad (3)$$

Hence H is the Lyapunov functional of (1). Equation (1) suggests that the order parameter $w(\mathbf{r},t)$ evolves in time with a typical wave number k_0. The dynamics for small ϵ reflects the ordering process in the Rayleigh-Bénard convection, where the velocity field is symmetric with respect to a plane if the upper and lower plates have the same boundary conditions [10].

The aim of the present paper is to show that the SH equation (1) exhibits a phase ordering kinetics similar to that studied in terms of the time-dependent Ginzburg-Landau (TDGL) equation

$$\frac{\partial\psi}{\partial t}=\epsilon\psi-\psi^3+\nabla^2\psi, \quad (4)$$

if $\epsilon>\epsilon_c$, where $\epsilon_c(>0)$ denotes a certain critical value being specified below. It is known that the latter system describes the ordering kinetics generated by a temperature quench from the disorderd phase ($\psi\simeq 0$) for $\epsilon<0$ to a two-phase region for $\epsilon>0$ [11,12].

Although the SH equation (1) was derived for a small $|\epsilon|$, we hereafter regard it as a model equation, and choose ϵ arbitrary. The SH has two nontrivial uniform states

$$w_0^{(\pm)}=\pm\sqrt{\epsilon-k_0^4} \quad (5)$$

for $\epsilon>k_0^4$, which are linearly stable for $\epsilon>3/2k_0^4\equiv\epsilon_c$ [13].

Let us first discuss the domain dynamics in one dimension. A steady kink pattern $w_*(\xi)$ satisfies

$$\left(\frac{d^2}{d\xi^2}+k_0^2\right)^2 w_*=\epsilon w_*-w_*^3, \quad (6)$$

with the condition $w_*(\pm\infty)=w_0^{(\pm)}$. The kink is located at $\xi=0$. The asymptotic solution of (6) sufficiently far away from the kink position is given by [13]

$$w_*(\xi)=w_0+A\ \exp(-|\xi|/\xi_0)\cos[Q(\xi-\phi)], \quad (7)$$

where A and ϕ are constants. ξ_0 and Q determine the kink width and the wave number of the wave front oscillation. They are given by

$$\xi_0=\left(\frac{2}{\sqrt{2(\epsilon-k_0^4)}-k_0^2}\right)^{1/2}, \quad Q=\{\tfrac{1}{2}[\sqrt{2(\epsilon-k_0^4)}+k_0^2]\}^{1/2}. \quad (8)$$

Figure 1 shows the numerically determined evolution of a

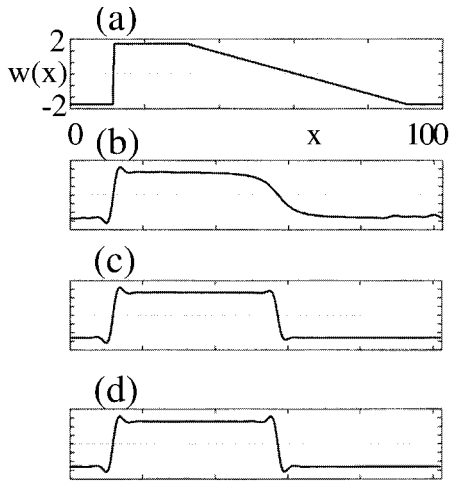

FIG. 1. Temporal evolution of kink-antikink pair observed at $\epsilon=2.7$ in the one-dimensional system for a given initial condition. Times are (a) $t=0$, (b) 1, (c) 2, (d) 50.

one-dimensional kink-antikink pair. The simulation has been carried out at $\epsilon=2.7$ and $k_0=1$. It has features similar to those of the TDGL equation with the exception that the present kink pattern oscillates near the interface of the domains due to the existence of the wave number k_0.

Hereafter we will study the domain dynamics in two dimensions numerically and analytically. The two uniform states (5) are stable for $\epsilon>\epsilon_c$, and an appropriate initial condition will lead to the phase separation. Since the roll pattern is stable also, the two patterns compete with each other. Hence the final pattern depends on the initial condition.

At first we have numerically solved (1) by making use of the explicit Euler scheme on a two-dimensional square lattice with a periodic boundary condition. The simulation was carried out with a time step $\Delta t=1/1600$ and a mesh size $\Delta x=\pi/8$. The initial state was generated by adding a random number uniformly distributed in the range $[-0.01, 0.01]$ to the unstable uniform state $w_0=0$.

Figures 2(a)–2(d) show typical spatial patterns for several values of ϵ/k_0^4 on a square lattice of grid size 256×256 at the time $t=200$. These figures reveal a specific property of the phase separation in the SH equation. For small ϵ/k_0^4, a roll state overcomes the uniform pattern, and one observes the roll pattern shown in Fig. 2(a). On the other hand, a uniform state is more stable than roll patterns for large ϵ/k_0^4, where one observes the phase separation as a transient process [Fig. 2(d)]. In addition, these figures suggest that there exists a threshold between both regimes. As will be discussed in the sequel, the threshold is evaluated as $\epsilon_{\rm cr}\simeq6.3k_0^4$. The value of the Lyapunov functional for the uniform solution w_0 is easily obtained as

$$H\{w_0\}=\tfrac{1}{4}(\epsilon-k_0^4)^2S, \tag{9}$$

where S is the area of the system. Values of the Lyapunov functional for nonuniform states are determined after a transient process in a simulation on a square lattice of grid size 128×128. Figure 3 shows the value of H for uniform solutions and those obtained from the numerical simulation at

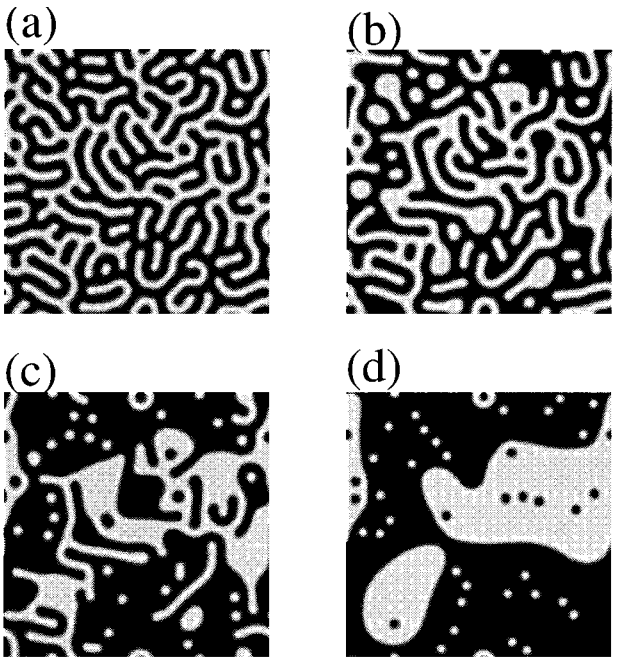

FIG. 2. Spatial patterns for (a) $\epsilon=4$, (b) 6.0, (c) 6.4, (d) 8 on a square lattice of grid size 256×256 with $t=200$. These figures suggest that there exists a threshold $\epsilon_{\rm cr}\simeq6.3k_0^4$ from a roll pattern to a uniform pattern. For details see the text.

time $t=1000$ as a function of ϵ. The figure suggests that there exist a threshold $\epsilon_{\rm cr}$ where both data cross each other. If $H\{w_{\rm roll}\}$ denotes the Lyapunov functional for the roll pattern, and $H\{w_{\rm spot}\}$ for the uniform state with spots then

$$\begin{aligned} H\{w_0\}&>H\{w_{\rm roll}\} \quad \text{for } \epsilon<\epsilon_{\rm cr},\\ H\{w_0\}&<H\{w_{\rm spot}\} \quad \text{for } \epsilon>\epsilon_{\rm cr}. \end{aligned} \tag{10}$$

Accordingly, the roll solution and the uniform solution are both stable for $\epsilon>3k_0^4/2$, but the roll solution is more stable for $\epsilon<\epsilon_{\rm cr}$ whereas the uniform solution is more stable for

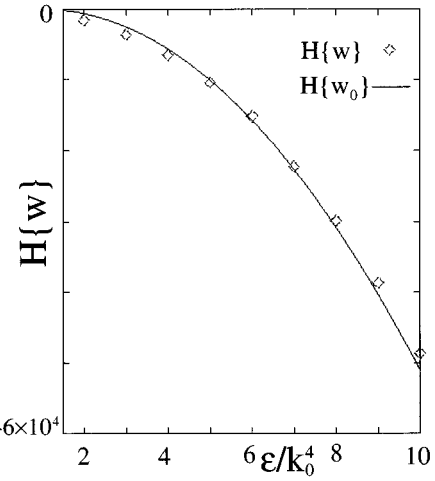

FIG. 3. The Lyapunov functional of the uniform solution (9) (solid line) and of numerical simulation (diamonds). The simulation was carried out on a square lattice of grid size 128×128 and values of the Lyapunov functional were evaluated at $t=1000$.

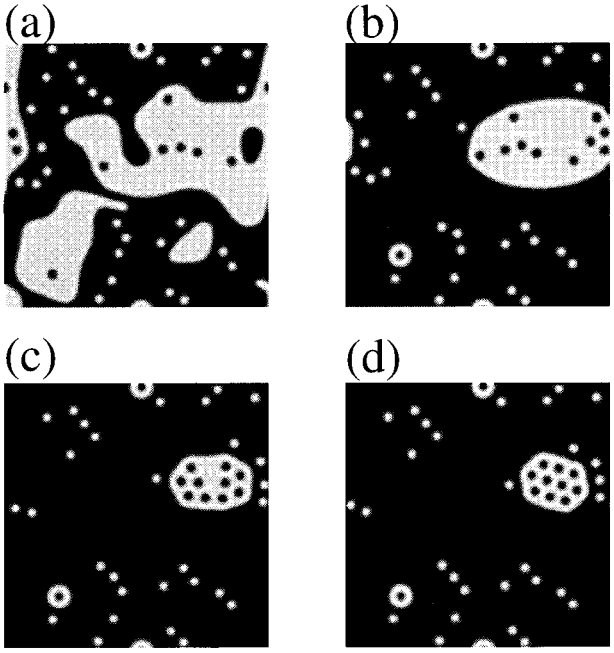

FIG. 4. Spatial patterns at (a) $t=100$, (b) 1000, (c) 2000, (d) 3000 with $\epsilon=8$. These figures reveal that the domain wall propagates so as to reduce the domain structure and eventually shrinks to a spot. The spot pattern coexists with the phase separation pattern.

$\epsilon>\epsilon_{\rm cr}$. As a result, the time evolution from the unstable uniform state leads to a roll pattern for $\epsilon<\epsilon_{\rm cr}$ and to a phase separation pattern for $\epsilon>\epsilon_{\rm cr}$. From that figure $\epsilon_{\rm cr}$ is estimated to be in the range $[5k_0^4,6k_0^4]$. However $\epsilon_{\rm cr}$ evaluated in this way is smaller than the value obtained from the direct observation of the pattern. This difference stems from the slow evolution of the Lyapunov functional so that the value at time $t=1000$ is insufficient to determine the final value. The determination from the direct observation of the pattern yields $\epsilon_{\rm cr}\simeq 6.3k_0^4$. This is consistent with the fact that the Lyapunov functional decreases as time goes on, which means that the crossing point of the solid line and the curve with diamonds in Fig. 3 may shift to the right.

The asymptotic behavior of the phase separation was studied numerically at $\epsilon=8k_0^4$. The simulation has been carried out on a square lattice of grid size 256×256, and the pattern evolution is observed for $0<t<3000$. Figure 4 shows a typical evolution of patterns at (a) $t=100$, (b) 1000, (c) 2000, and (d) 3000. The domain wall propagates, reduces the domain structure, and finally shrinks to one spot, provided that there was no spot present in the inital domain. If several spots are enclosed by a domain wall, the shrinking process does not destroy the spots but forms the ''lotus root'' structure shown in Fig. 4(d). Once such a structure is created, it appears to remain unchanged indicating that it is a metastable structure. Our simulations were carried out up to a time $t=3000$, and we infer that the structure is metastable at least on this time scale.

Let us discuss the propagation velocity $c(R)$ of the domain wall in dependence on the curvature radius R, which is assumed to be large compared to the width of the kink. Assuming an axial symmetry of the pattern, (1) is approximately written in polar coordinates

$$\frac{\partial w}{\partial t}=\epsilon w-\left(\frac{\partial^2}{\partial r^2}+k_0^2\right)^2 w-\frac{2}{R}w'''-\frac{2k_0^2}{R}w'-w^3. \quad (11)$$

The primes denote derivatives with respect to the radial coordinate r. In deriving this expression we have replaced the Laplacian ∇^2 by $\partial^2/\partial r^2+(1/R)\partial/\partial r$ for the large radius of the domain wall R, and we have neglected terms of order R^{-2}. With this approximation the trigger wave is described by a solution $w=w(\eta)$ with $\eta=r-c(R)t$, where the speed c of the wave front is determined by the differential equation

$$-\left[c(R)-\frac{2}{R}\frac{w'''}{w'}-\frac{2k_0^2}{R}\right]w'=\epsilon w-\left(\frac{\partial^2}{\partial r^2}+k_0^2\right)^2 w-w^3. \quad (12)$$

Taking Eq. (6) into account we find that the speed obeys

$$c(R)=\frac{2}{R}\left(k_0^2+\left.\frac{w'''}{w'}\right|_R\right). \quad (13)$$

The explicit value of the velocity $c(R)$ can be obtained as follows. First the term $w'''/w'|_R$ is determined by using the amplitude equation of the one-dimensional SH equation. By noting that (1) has a characteristic wave number k_0, the solution of (1) in one dimension is approximately expressed in the form

$$w(x,t)={\rm Re}[e^{ik_0x}\Psi(x,t)]. \quad (14)$$

Substituting (14) into (1), one obtains the TDGL equation

$$\frac{\partial\Psi}{\partial t}=\epsilon\Psi-|\Psi|^2\Psi+4k_0^2\frac{\partial^2\Psi}{\partial x^2}. \quad (15)$$

The stationary solution with the boundary condition $\Psi(\pm\infty)=\pm\sqrt{\epsilon}$ is given by [14]

$$\Psi(x)=\sqrt{\epsilon}\,\tanh\left(\left[\frac{\epsilon}{8k_0^2}\right]^{1/2}x\right). \quad (16)$$

Inserting solution (16) into (14), the explicit value of $w'''/w'|_R$ at $x=0$ reads $w'''/w'|_R=-(\epsilon+12k_0^4)/4k_0^2$. Then the propagation velocity $c(R)$ of the domain wall takes the explicit form

$$c(R)=-\frac{2}{R}\frac{\epsilon+8k_0^4}{4k_0^2}. \quad (17)$$

The direction of the propagation coincides with the simulation result. Namely, the domain wall propagates so as to reduce the domain structure.

Furthermore, to investigate the relaxation dynamics for $\epsilon>\epsilon_{\rm cr}$, let us introduce the structure function $S(k,t)$ of $w(\mathbf{r},t)$ by

$$S(k,t)=\left\langle\left|\int\int w(\mathbf{r},t)e^{i\mathbf{k}\cdot\mathbf{r}}dx\,dy\right|^2\right\rangle, \quad (18)$$

where $k=|\mathbf{k}|$ and $\langle\cdots\rangle$ denotes the average taken with respect to the orientation of $\mathbf{k}$. One gets the statistical characteristics of the ordering process by observing the time dependence of $S(k,t)$. In our case $S(k,t)$ has a single peak with

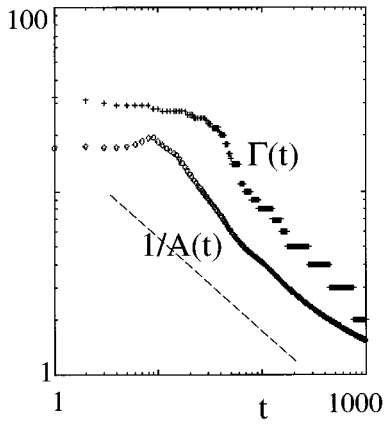

FIG. 5. Time evolution of the peak height $A(t)$ and the peak width $\Gamma(t)$ of the structure function $S(k,t)$ for $\epsilon=8$. They show a power law $A(t)\propto t^{\beta}$, $w(t)\propto t^{-\beta}$ with $\beta=1/2$.

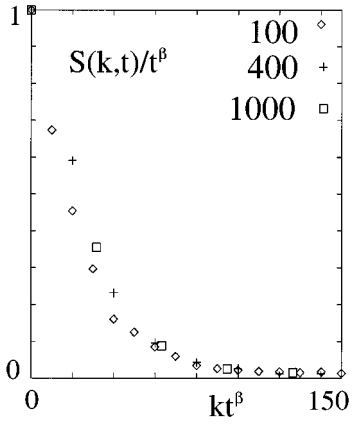

FIG. 6. Scaling plot of $S(k,t)/t^{\beta}$ vs kt^{β} with $\beta=1/2$ for $\epsilon=8$ at $t=100$, 400 and 1000. This figure reveals that $S(k,t)$ is asymptotically scaled as $S(k,t)=t^{\beta}g(kt^{\beta})$ with a scaling function $g(z)$.

amplitude $A(t)$ and width $\Gamma(t)$, where the latter is defined as $S(\Gamma(t),t)=e^{-1}A(t)$. $\Gamma(t)$ and $1/A(t)$ are plotted as functions of t in Fig. 5. In an intermediate time region corresponding to the phase order, $A(t)$ and $\Gamma(t)$ appear to depend on t as

$$A(t)\propto t^{\beta}, \quad \Gamma(t)\propto t^{-\beta}, \tag{19}$$

with the dynamic scaling exponent β, where β takes approximately the value 1/2. We will comment on the deviations from this behavior at the end of this paragraph. Figure 6 shows $S(k,t)/t^{\beta}$ vs kt^{β} at $t=100$, 400, and 1000. This implies that in the above mentioned intermediate region, a scaling law

$$S(k,t)=t^{\beta}g(kt^{\beta}) \tag{20}$$

appears to hold, where $g(x)$ is a scaling function. The same scaling relationship is known from the TDGL equation. It has been found that the scaling function of the SH equation for a small $\epsilon(>0)$ has its maximum at $k=k_0$ because of the existence of the spatial structure, and the scaling exponent takes the value $\beta=1/5$ [15]. Figure 6, on the other hand, shows that the scaling function for $\epsilon>\epsilon_{\rm cr}$ has no peak, and that the dynamics of the phase separation evolves much faster compared to the formation process of roll patterns. However, in the stage following the separation, the ''lotus root'' structure shown in Fig. 4(d) dominates the dynamics, which causes an extremely slow relaxation dynamics. Figure 5 suggests that the temporal evolution with the ''lotus root'' structure is slower than that of the phase separation mentioned above.

The asymptotic dynamics observed in the formation of the ''lotus root'' structure appears to have two different length scales, i.e., the scale of the phase separation and that of the ''lotus root'' structure (cf. Fig. 4). The coexistence of these length scales of structures makes the dependence (19) on t difficult to observe. When our simulation is performed with a larger system size, it is expected that the intermediate time region, where the length scale of the phase separation is much larger than that of the ''lotus root'' structure, tends to increase. Hence the dependence (19) on t is more pronounced. The analysis of the dependence (19) and the value of β are the matter of future investigation.

The authors are grateful to W. Just for a critical reading of the manuscript. This study was partially supported by a Grant-in-Aid for General Scientific Research (No. 40156849) from the Ministry of Education and Culture, Japan.

[1] P. Manneville, *Dissipative Structures and Weak Turbulence* (Academic, Boston, 1990).
[2] For reviews on formation dynamics far from equilibrium, see M. C. Cross and P. C. Hohenberg, Rev. Mod. Phys. **65**, 851 (1993).
[3] P. G. de Gennes, *Physics of Liquid Crystals* (Clarendon, Oxford, 1982).
[4] S. Chandrasekhar, *Liquid Crystals* (Cambridge University Press, Cambridge, England, 1977).
[5] E. Meron, Phys. Rep. **218**, 1 (1992).
[6] Q. Ouyang and H. L. Swinney, Nature **352**, 610 (1991).
[7] M. Bestehorn and C. Pérez-Garcia, Physica D **61** 67 (1992).
[8] J. Verdasca, A. De Wit, G. Dewel, and P. Borckmans, Phys. Lett. A **168**, 194 (1992).
[9] K. Ouchi, T. Horita, K. Egami, and H. Fujisaka, Physica D **71**, 367 (1994).
[10] J. Swift and P. C. Hohenberg, Phys. Rev. A **15**, 319 (1977).
[11] J. D. Gunton, M. S. Miguel, and P. S. Sahni, *Phase Transitions and Critical Phenomena* (Academic, New York, 1983).
[12] H. Furukawa, Adv. Phys. **34**, 703 1985.
[13] H. Fujisaka, K. Ouchi, and K. Egami (unpublished).
[14] P. M. Chaikin and T. C. Lubensky, *Principles of Condensed Matter Physics* (Cambridge University Press, Cambridge, England, 1995).
[15] K. R. Elder, J.Viñals, and M. Grant, Phys. Rev. Lett. A **46**, 7618 (1992).